Synthesis and application of tin triflate-containing MCM-41 as heterogeneous Lewis acid catalysts for the Mukaiyama aldol reaction at room temperature

Masakazu Saito · Hikaru Ikeda · Yu Horiuchi · Masaya Matsuoka

Abstract Sn-containing MCM-41 (Sn-MCM-41) with different tin content was prepared by hydrothermal synthesis then treated with triflic acid to form tin triflate within the silica framework (SnOTf-MCM-41). XRD and UV–visible measurements revealed that SnOTf-MCM-41 have highly ordered mesoporous structures with tetrahedrally-coordinated Sn species. Moreover, results from FT-IR analysis revealed that triflate ligands are selectively coordinated with Sn^{4+} species in the mesoporous silica frameworks. SnOTf-MCM-41, as Lewis acid catalysts, promoted the Mukaiyama aldol reaction of benzaldehyde with 1-trimethylsiloxycyclohexene at room temperature and had greater catalytic activity than untreated Sn-MCM-41. Taking into account results from in situ FT-IR experiments using pyridine as probe molecule, the enhanced catalytic performance after triflic acid treatment was attributed to an increase in the number of acid sites, because of appearance of water tolerance by the formation of metal triflate species. In addition, the SnOTf-MCM-41 catalyst was reusable at least three times in the Mukaiyama aldol reaction.

Keywords Tin triflate-containing MCM-41 · Lewis acid · Mukaiyama aldol reaction · Reusability

Introduction

Lewis acid metal halides, for example $AlCl_3$, $FeCl_3$, and $ZnCl_2$, are widely used as homogeneous catalysts for industrial organic synthesis, because of their low cost and ready availability. These acids have disadvantages, however, including: use of the metal halides in stoichiometric or greater amounts; generation of large amounts

M. Saito · H. Ikeda · Y. Horiuchi · M. Matsuoka (✉)
Department of Applied Chemistry, Graduate School of Engineering, Osaka Prefecture University,
1-1 Gakuen-cho, Naka-ku, Sakai, Osaka 599-8531, Japan
e-mail: matsumac@chem.osakafu-u.ac.jp

of aqueous effluents during the post-synthesis work-up; and the difficulty of recovering the catalysts from the effluent for reuse.

To solve these issues, many researchers have focused on heterogeneous catalytic systems which enable recovery the catalysts after the end of the reaction and their reuse for further catalytic cycles. However, because the performance of heterogeneous catalysts is often inferior to that of homogeneous catalysts under the same reaction conditions, development of highly active heterogeneous catalysts is required.

Recently, Corma and co-workers [1] reported that Ti-containing mesoporous silica catalysts have high catalytic activity in heterogeneous Mukaiyama aldol reactions. Silica-based porous materials, for example mesoporous silicas and zeolites, are characterized by high specific surface area, chemical resistance, and ease of incorporation of different metal species [1–7]. Therefore, these porous materials are often used as catalyst supports. Compared with Ti^{4+} ions, Sn^{4+} ions incorporated into MFI-type zeolites are more acidic and have greater catalytic activity in the dehydration of cyclohexanol [7]. However, the strong Lewis acid sites are easily deactivated in water by hydration [8]. In this context, Kobayashi et al. [8–10] reported that homogeneous metal triflate catalysts can be used as Lewis acid catalysts in the presence of water. This water tolerance was related to the lower nucleophilicity of their triflate (OTf) ligands. Thus, Sn-containing silica-based porous catalysts are expected to have high Lewis acid catalytic activity as a result of coordination of Sn^{4+} with OTf ligands.

In this study, Sn-containing MCM-41 with different tin content (Sn_x-MCM-41; $x = 1.4$, 5.5, and 6.7 % w/w) were prepared by hydrothermal synthesis then treated with triflic acid to form tin triflate within the silica framework (Sn_xOTf-MCM-41), by following the methods reported by Coman and co-workers [11–14]. Sn_xOTf-MCM-41 were used in the Mukaiyama aldol reaction of benzaldehyde with 1-trimethylsiloxycyclohexene at room temperature as model Lewis acid-catalyzed reaction. Moreover, FT-IR analysis using pyridine as probe molecule was performed for evaluation of the acid sites.

Experimental

Synthesis of Sn_xOTf-MCM-41

Sn_xOTf-MCM-41 were prepared via synthesis of Sn_x-MCM-41 then triflic acid treatment. First, Sn_x-MCM-41 with tin content of 1.4, 5.5, and 6.7 % (w/w) were synthesized by a hydrothermal method [3, 15]. A given amount of $SnCl_4 \cdot 5H_2O$ was dissolved in 15 mL distilled water and mixed with 16.7 g cetyltrimethylammonium chloride (CTMACl) as structure template. After dissolution of the CTMACl, 2.08 g tetramethylammonium hydroxide and 12.5 mL distilled water were added. Tetramethylammonium silicate (13.6 g) was then added dropwise to the solution, which was stirred for 20 min, then fumed silica (3.1 g) was added slowly and the suspension obtained was stirred for 1 h. The resulting mixture was transferred to a stainless-steel autoclave and aged in an oven at 393 K for 5 days under static

conditions, to complete the crystallization. The resulting product was isolated by filtration, washed with distilled water, dried at 373 K for 12 h, then calcined at 823 K for 8 h in air to remove residual structure template, yielding Sn_x-MCM-41 as a white powder. This was then treated in a triflic acid solution [11–14]. Typically, 2 g Sn_x-MCM-41 was stirred under reflux at 353 K for 15 h in triflic acid solution (5 g triflic acid in 50 mL methanol). The resulting white powder was collected by filtration, washed adequately with methanol to eliminate excess triflic acid on the silica surface, and dried at 353 K for 12 h. The samples obtained were designated Sn_xOTf-MCM-41 ($x = 1.4$, 5.5, and 6.7 % w/w).

Characterization of Sn_xOTf-MCM-41

X-ray diffraction (XRD) patterns were acquired by means of a Shimadzu XRD-6100 using Cu Kα radiation ($\lambda = 1.5406$ Å). Diffuse reflectance UV–visible spectra were obtained by use of a Shimadzu UV-2200A spectrophotometer. FT-IR spectra were recorded with 4 cm^{-1} resolution, in transmission mode, by use of a Jasco FT-IR 660 Plus; samples were pressed into self-supported disks (1 cm^2 area, 12 mg cm^{-2}). In situ FT-IR experiments were also performed, using pyridine as molecular probe for evaluation of acid properties. Before measurements, the sample disks were degassed at 373 K for 2 h in vacuo and treated with saturated pyridine vapor at room temperature for 30 min followed by evacuation at 373 K for 30 min to remove physisorbed pyridine. The pyridine-adsorbed FT-IR spectra were then collected at room temperature. The difference spectra were obtained by subtracting reference spectra collected before pyridine adsorption.

Heterogeneous Mukaiyama aldol reaction

Heterogeneous Mukaiyama aldol reaction of benzaldehyde with 1-trimethylsiloxycyclohexene were performed in a glass vessel equipped with a vacuum line connector. The catalyst (30 mg) was placed in the glass vessel and pretreated at 373 K for 2 h in vacuo. After replacement with Ar atmosphere, 5 mL dry toluene, 1.0 mmol benzaldehyde, and 1.2 mmol 1-trimethylsiloxycyclohexene were added to the glass vessel. Reactions were conducted at room temperature for 3 h with stirring. After the reaction, 0.33 mmol 9-methylanthracene was added to the reaction mixture as an index for ^{1}H NMR. The catalyst and toluene were removed by filtration and evaporation, respectively. Substances were analyzed by ^{1}H NMR. The turnover number (TON) was defined as follows:

$$TON = [\text{moles of aldol products}]/[\text{mole of Sn in the catalyst}]$$

Results and discussion

The XRD patterns of Sn_xOTf-MCM-41 and pure silica MCM-41 are given in Fig. 1. All diffraction patterns were almost the same as those of the MCM-41 materials reported by Beck et al. [2]. A sharp diffraction peak was observed at $\theta = 2–2.5°$ in

all patterns; this was ascribed to the (100) reflection of hexagonal mesopores. Besides the strong peak, the patterns contained weak diffraction peaks at $3^o < 2\theta < 7^o$ ascribed to (110), (200), and (210) reflections of the mesopores. In addition, the surface area of $Sn_{5.5}$-MCM-41 and $Sn_{5.5}$OTf-MCM-41, determined by use of N_2 adsorption–desorption isotherms, were 1107 and 924 m^2 g^{-1}, respectively. These results reveal that the mesoporous structures were retained even after incorporation of tin triflate into the MCM-41 frameworks. The observable peak shift to higher angle with increasing tin content implies that the pore size became narrower, because of the larger ionic radius of Sn^{4+} compared with Si^{4+}. No diffraction peaks ascribed to tin compounds, for example crystalline tin oxide, were observed in the high-angle region, implying that the Sn within the silica framework exists in a highly dispersed state, with no formation of aggregated species.

Diffuse reflectance UV–visible spectroscopy is a very sensitive means of detection of the coordination state of Sn species [15, 16]. It is also an ideal technique for verifying incorporation of tin into the MCM-41 structure. Figure 2 shows the UV–visible diffuse reflectance spectra of Sn_xOTf-MCM-41. For comparison, the spectra of bulk SnO_2 and pure silica MCM-41 are also included in Fig. 2. The bulk SnO_2 spectrum contains a broad absorption peak at approximately 284 nm, assigned to hexacoordinated polymeric Sn–O–Sn type species [15, 16], whereas almost no absorption band in this region is observed for MCM-41. The spectra of all Sn_xOTf-MCM-41 contained an absorption band at approximately 208 nm, suggesting the presence of Sn^{4+} in tetrahedral coordination within the silica frameworks of Sn_xOTf-MCM-41 [15, 16]. In addition, the peak intensity at approximately 208 nm was found to increase with increasing tin content of Sn_xOTf-MCM-41. However, the broader character of the peak from 208 to 300 nm may be associated with the presence of site-isolated Sn species in a distorted tetrahedral environment or in penta or octahedral coordination spheres [15].

Figure 3 shows the FT-IR spectra of $Sn_{5.5}$-MCM-41 and pure silica MCM-41 before and after triflic acid treatment. The FT-IR spectrum of tin triflate is also included in Fig. 3 for reference. The spectra of $Sn_{5.5}$-MCM-41 and MCM-41 clearly contain vibrational bands of v_{as}(Si–O–Si), v_s(Si–O–Si), and δ(Si–O–Si) at 1,085, 800, and 455 cm^{-1}, respectively [17, 18]. After triflic acid treatment, new vibration bands appeared at 1,269, 1,210, and 785 cm^{-1}, attributed to CF_3 vibrations of $Sn_{5.5}$OTf-MCM-41; new bands at 1,179, 1,035, and 645 cm^{-1} were attributed to S=O and S–O vibrations, respectively, and were coincident with those in the spectrum of tin triflate [19]. These results suggest that tin triflate is successfully formed within the porous silica frameworks by post-synthesis triflic acid treatment. In contrast, no significant change was observed in the spectrum of pure silica MCM-41 after triflic acid treatment. These findings indicate that the OTf ligands are selectively coordinated with Sn sites in the Sn_x-MCM-41.

In an investigation of the potential catalytic activity of Sn_x-MCM-41 and Sn_xOTf-MCM-41, heterogeneous Mukaiyama aldol reactions of benzaldehyde with 1-trimethylsiloxycyclohexene were performed at room temperature (Scheme 1). Mukaiyama aldol reactions catalyzed by Lewis acids enable reaction of an aldehyde with a silyl enolate [1]. As shown in Table 1, Sn_x-MCM-41 and Sn_xOTf-MCM-41
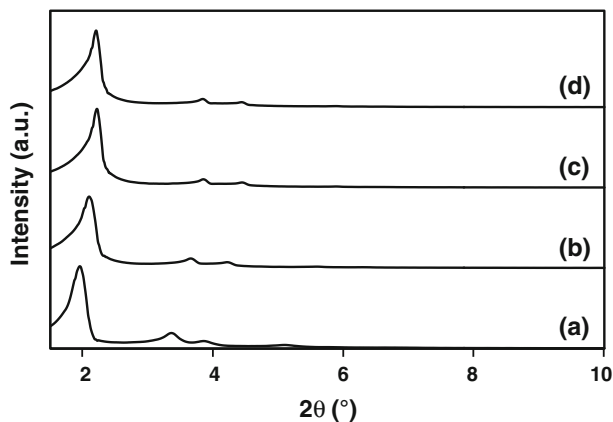
Fig. 1 XRD patterns of **a** MCM-41 and **b–d** Sn$_x$OTf-MCM-41 with tin content of **b** 1.4, **c** 5.5, and **d** 6.7 % (*w/w*)
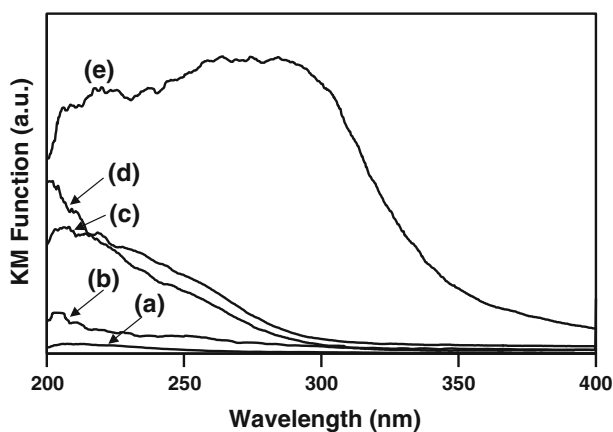

Fig. 2 Diffuse reflectance UV–visible spectra of: **a** MCM-41; **b–d** Sn$_x$OTf-MCM-41 with tin content of **b** 1.4, **c** 5.5, and **d** 6.7 % (*w/w*); and **e** SnO$_2$

had catalytic activity in the Mukaiyama aldol reaction, giving the *syn* product with high selectivity, whereas bulk SnO$_2$ and pure silica MCM-41 hardly promoted this reaction under the same reaction conditions. Yields of the products increased with increasing tin content of Sn$_x$-MCM-41 and Sn$_x$OTf-MCM-41. However, the TON of Sn$_{6.7}$-MCM-41 and Sn$_{6.7}$OTf-MCM-41 were lower than that of the catalyst with tin content of 5.5 % (*w/w*), because the ratio of tetrahedrally coordinated Sn species acting as Lewis acid sites decreases with increasing tin content above 5–6 % (*w/w*) in Sn$_x$-MCM-41 and Sn$_x$OTf-MCM-41. Thus, the optimum tin content is approximately 5.5 % (*w/w*). Furthermore, Sn$_x$OTf-MCM-41 had much higher catalytic activity than Sn$_x$-MCM-41, indicating that the Lewis acid property of tetrahedrally coordinated Sn species can be enhanced by coordination of Sn^{4+} with OTf ligands. Interestingly, Sn$_{5.5}$-MCM-41 pretreated at 573 K for 2 h in vacuo
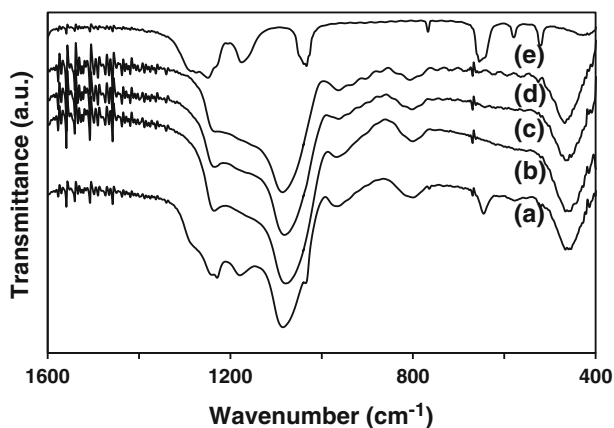
Fig. 3 FT-IR spectra of: **a, b** $Sn_{5.5}$-MCM-41 and **c, d** MCM-41 before (**b, d**) and after (**a, c**) triflic acid treatment; **e** tin triflate

before use in the reaction had catalytic activity similar to that of $Sn_{5.5}$OTf-MCM-41 (entry 7). Considering that the pretreatment helps to remove adsorbed water molecules that suppress the Lewis acidity of Lewis acid sites, coordinating OTf ligands should prevent adsorption of water molecules by tetrahedrally coordinated Sn species. MCM-41-supported $Sn(OTf)_2$, ($Sn(OTf)_2$/MCM-41, 5.5 % *w/w* Sn), which was prepared by an impregnation method using an ethanol solution of $Sn(OTf)_2$ and MCM-41, had no *syn/anti* selectivity (entry 8). This finding indicates that the presence of tetrahedrally coordinated Sn species is responsible for high *syn* selectivity.

To gain insight into the detailed reason for the enhancement of catalytic ability, in situ FT-IR experiments were performed using pyridine as probe molecule for acid sites. The pyridine adsorption technique is used for assessment of Brønsted and Lewis acidity [20]. Figure 4 shows the difference FT-IR spectra of pyridine-adsorbed MCM-41, $Sn_{5.5}$-MCM-41, and $Sn_{5.5}$OTf-MCM-41. For comparison, the spectrum of $Sn_{5.5}$-MCM-41 pretreated at 573 K for 2 h in vacuo is also shown in Fig. 4. The spectra of $Sn_{5.5}$-MCM-41 and $Sn_{5.5}$OTf-MCM-41 contained typical bands at $\sim 1{,}455$ and $\sim 1{,}616$ cm^{-1}, assigned to pyridine adsorbed on Lewis acid sites, whereas MCM-41 contained no absorption band in this region. These results indicate that the Lewis acid sites are formed by incorporation of Sn species. The intensities of the peaks at 1,455 and 1616 cm^{-1} in the spectrum of $Sn_{5.5}$OTf-MCM-41 were higher than those in the spectrum of $Sn_{5.5}$-MCM-41, and almost the same as those in the spectrum of $Sn_{5.5}$-MCM-41 pretreated at 573 K. This result suggests that $Sn_{5.5}$OTf-MCM-41 contains a large number of effective Lewis acid sites even after pretreatment at low temperature (373 K), which is consistent with the results of the catalytic reaction. In addition, taking into account the fact that the number of Lewis acid sites in $Sn_{5.5}$OTf-MCM-41 is equal to that in $Sn_{5.5}$-MCM-41 pretreated at 573 K, almost all Lewis acid sites in $Sn_{5.5}$OTf-MCM-41 should be protected from adsorption of water molecules by the coordinating OTf ligands, that is, tetrahedrally coordinated Sn species should be coordinated with at least one OTf ligand. In the
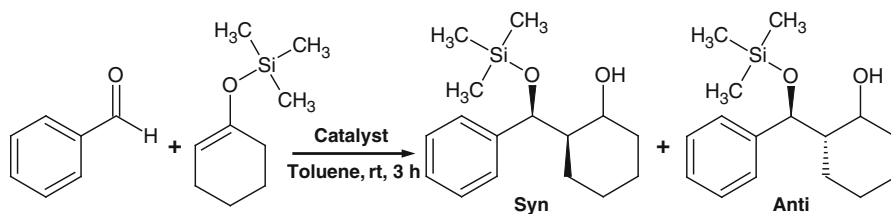
Scheme 1 Mukaiyama aldol reaction of benzaldehyde with 1-trimethylsiloxycyclohexene

Table 1 Mukaiyama aldol reaction of benzaldehyde with 1-trimethylsiloxycyclohexene and use of different solid acid catalysts

Entry	Catalyst	Sn content (% w/w)	Yield (%)[b]	TON[c]	Selectivity (%)	
					syn	*anti*
1	Sn-MCM-41	1.4	1.2	3.4	100	0
2	Sn-MCM-41	5.5	27.5	19.8	98	2
3	Sn-MCM-41	6.7	31.5	18.5	98	2
4	SnOTf-MCM-41	1.4	4.5	12.8	85	15
5	SnOTf-MCM-41	5.5	57.8	42.2	97	3
6	SnOTf-MCM-41	6.7	58.5	34.4	97	3
7	Sn-MCM-41[a]	5.5	55.6	40.198	2	
8	Sn(OTf)2/MCM-41	5.5	59.4	42.9	50.6	49.4
9	MCM-41	–	n.d.	–	–	–
10	SnO$_2$	78.8	n.d.	–	–	–

[a] Pretreated at 573 K for 2 h in vacuo before use in the reaction

[b] Yield of aldol products

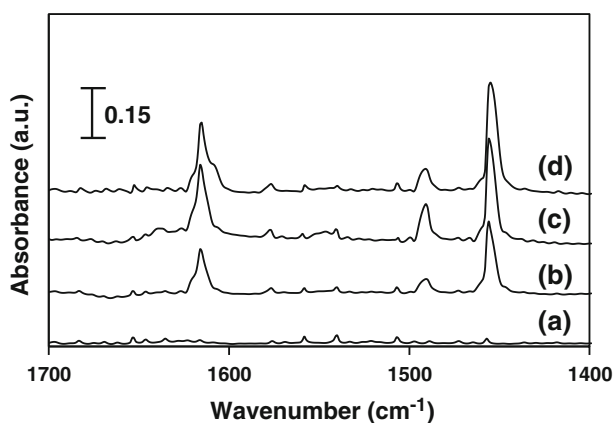[c] Turnover number (TON) = (moles of aldol products)/(moles of Sn in the catalyst)

Fig. 4 Difference FT-IR spectra of pyridine adsorbed on **a** MCM-41, **b** Sn$_{5.5}$-MCM-41, **c** Sn$_{5.5}$OTf-MCM-41 pretreated at 373 K before pyridine adsorption, and **d** Sn$_{5.5}$-MCM-41 pretreated at 573 K before pyridine adsorption
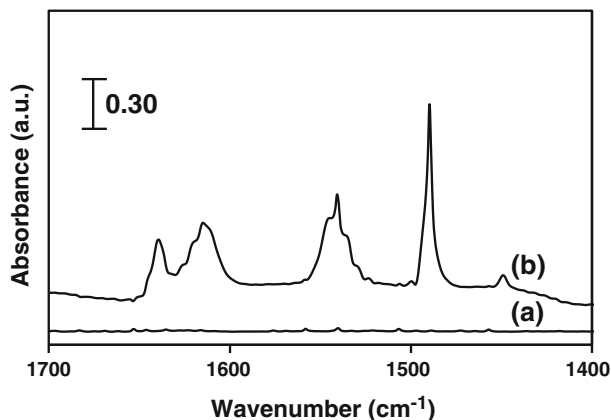
Fig. 5 Difference FT-IR spectra of pyridine adsorbed on **a** MCM-41 and **b** Sn(OTf)$_2$/MCM-41
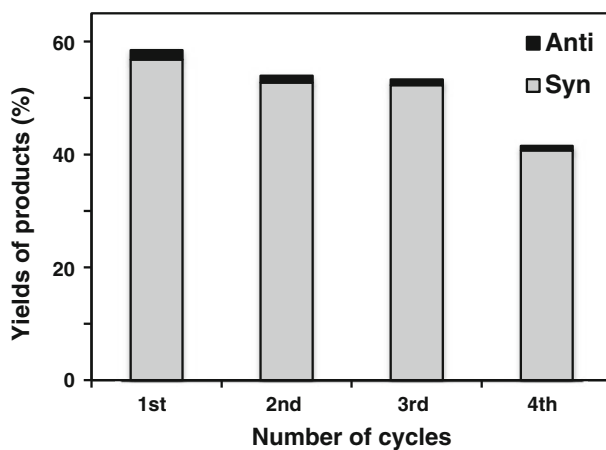

Fig. 6 Mukaiyama aldol reaction of benzaldehyde with 1-trimethylsiloxycyclohexene over Sn$_{5.5}$OTf-MCM-41, and recycling results

homogeneous systems, the metal salt of triflic acid or metal triflates (M(CF$_3$SO$_2$)$_n$ or M(OTf)$_n$) fall into an interesting category of catalysts with high Lewis acidity and water tolerance [21]. It is, therefore, believed that the coordinating OTf ligands bring about water tolerance to tetrahedrally coordinated Sn species as Lewis acid sites. It is also worth noting that the spectrum of Sn(OTf)$_2$/MCM-41 contained typical bands at $\sim 1,640$ and $\sim 1,540$ cm^{-1}, assigned to pyridine adsorbed on Brønsted acid sites, and at $\sim 1,455$ and $\sim 1,616$ cm^{-1}, assigned to pyridine adsorbed on Lewis acid sites, as shown in Fig. 5. This result implies that Sn(OTf)$_2$/MCM-41 contains not only Lewis acid sites but also Brønsted acid sites. The Brønsted acid sites may account for its low selectivity. A detailed study of the reaction mechanisms is now in progress.

Finally, the reusability of the $Sn_{5.5}OTf$-MCM-41 catalyst for the heterogeneous Mukaiyama aldol reaction was investigated under the same reaction conditions. The catalyst was recovered from the reaction mixture by filtration, then dried at 373 K for 4 h in air. As shown in Fig. 6, $Sn_{5.5}OTf$-MCM-41 had almost the same catalytic activity for three catalytic cycles, suggesting that the tin triflates were stably incorporated within the mesoporous silica framework and were not leached during the reactions.

Conclusions

Tin triflate-containing MCM-41 with different tin content (Sn_xOTf-MCM-41; x = 1.4, 5.5, and 6.7 % w/w) were successfully prepared by two-step synthesis. In the first step, Sn-containing mesoporous silicas (Sn_x-MCM-41) were prepared by use of a conventional hydrothermal method. The Sn_x-MCM-41 obtained were then treated with triflic acid to form tin triflate within the silica frameworks. Characterization studies revealed the synthesized Sn_xOTf-MCM-41 had highly ordered mesoporous structures and that the Sn species were selectively tetrahedrally coordinated by OTf ligands in the silica frameworks. Sn_xOTf-MCM-41 had greater catalytic activity than Sn_x-MCM-41 in the Mukaiyama aldol reaction of benzaldehyde with 1-trimethylsiloxycyclohexene. This is attributed to an increase in the number of effective Lewis acid sites as a result of coordination of Sn^{4+} with OTf ligands, because the OTf ligands confer water tolerance on tetrahedrally coordinated Sn species. Furthermore, the $Sn_{5.5}OTf$-MCM-41 catalyst could be reused at least three times in Mukaiyama aldol reactions.

References

1. R. Garro, M.T. Navarro, J. Primo, A. Corma, J. Catal. **233**, 342 (2005)
2. J.S. Beck, J.C. Vartulli, W.J. Roth, M.E. Leonowicz, C.T. Kresge, K.D. Schmitt, C.T.-W. Chu, D.H. Olson, E.W. Sheppard, S.B. McCullen, J.B. Higgins, J.L. Schlenker, J. Am. Chem. Soc. **114**, 10834 (1992)
3. T.K. Das, K. Chaudhari, A.J. Chandwadkar, S. Sivasanker, J. Chem. Soc. Chem. Commun. **196**, 2495 (1995)
4. R. Kumar, P. Vincent, K.V. Srinivasan, V.N. Raju, M. Sasidharan, Chem. Commun. 129 (1996)
5. M. Sasidharan, R. Kumar, Catal. Lett. **38**, 251 (1996)
6. M. Sasidharan, R. Kumar, J. Catal. **220**, 326 (2003)
7. N.K. Mal, A.V. Ramaswamy, J. Mol. Catal. A **105**, 149 (1996)
8. S. Kobayashi, I. Hachiya, J. Org. Chem. **59**, 3590 (1994)
9. K. Manabe, Y. Mori, T. Wakabayashi, S. Nagayama, S. Kobayashi, J. Am. Chem. Soc. **122**, 7202 (2000)
10. S. Kobayashi, K. Manabe, Acc. Chem. Res. **35**, 209 (2002)
11. S.M. Coman, G. Pop, C. Stere, V.I. Parvulescu, J.E. Haskouri, D. Beltran, P. Amoros, J. Catal. **251**, 388 (2007)
12. N. Candu, S.M. Coman, V.I. Parvulescu, J.E. Haskouri, P. Amoros, D. Beltran, Top. Catal. **52**, 571 (2009)
13. V.I. Parvulescu, S.M. Coman, N. Candu, J.E. Haskouri, D. Beltran, P. Amoros, J. Mater. Sci. **44**, 6693 (2009)

14. M. Verziu, J.E. Haskouri, D. Beltran, P. Amoros, D. Macovei, N.G. Gheorghe, C.M. Teodorescu, S.M. Coman, V.I. Parvulescu, Top. Catal. **53**, 763 (2010)
15. T.R. Gaydhankar, P.N. Joshi, P. Kalita, R. Kumar, J. Mol. Catal. A **265**, 306 (2007)
16. K. Chaudhari, T.K. Das, P.R. Rajmohanan, K. Lazar, S. Sivasanker, A. Chandwadkar, J. Catal. **183**, 281 (1999)
17. M.D. Alba, Z.H. Luan, J. Klinowski, J. Phys. Chem. **100**, 2178 (1996)
18. C.A. Koh, R. Nooney, S. Tahir, Catal. Lett. **47**, 199 (1997)
19. L.E. Fernandez, A.B. Altabef, E.L. Varetti, Spectrochim. Acta A **52**, 287 (1996)
20. S. Endud, K.L. Wong, Micropor. Mesopor. Mater. **101**, 256 (2007)
21. E. Altman, G.D. Stefanidis, T.V. Gerven, A. Stankiewicz, Ind. Eng. Chem. Res. **51**, 1612 (2012)